We are IntechOpen,
the world's leading publisher of
Open Access books
Built by scientists, for scientists

6,900
Open access books available

185,000
International authors and editors

200M
Downloads

154
Countries delivered to

Our authors are among the

TOP 1%
most cited scientists

12.2%
Contributors from top 500 universities

BOOK CITATION INDEX
CLARIVATE ANALYTICS
INDEXED

WEB OF SCIENCE™

Selection of our books indexed in the Book Citation Index
in Web of Science™ Core Collection (BKCI)

Interested in publishing with us?
Contact book.department@intechopen.com

Numbers displayed above are based on latest data collected.
For more information visit www.intechopen.com

5

Environmentally Assisted Cracking Behavior of Low Alloy Steels in Simulated BWR Coolant Conditions

J. Y. Huang, J. J. Yeh, J. S. Huang and R. C. Kuo
Institute of Nuclear Energy Research (INER), Chiaan Village, Lungtan,
Taiwan

1. Introduction

SA533, low carbon and low alloy steel, is most commonly used for nuclear reactor pressure vessels (RPV) whose integrity governs the safety of nuclear power plants. Fatigue is one of the main degradation mechanisms affecting the pressure vessel integrity of pressurized water reactors (PWRs) and boiling water reactors (BWRs) (Shah, 1993；Huang, 2001, 1999, 2007；Seifert, 2001, 2003). Fatigue life can generally be divided into two distinct phases－initiation and propagation. The factors affecting the initiation and propagation lives may not be the same. Recent test data indicate the initiation life is significantly decreased when the applied strain range, temperature, DO level in water, sulfur content in steel and strain rate are simultaneously satisfied(Chopra, 1997). The fatigue crack growth rates of RPV materials in simulated light water reactor (LWR) coolant environments are influenced by sulfur content, sulfide morphology (Huang, 2003, 2004；Van Der Sluys, 1985；Combrade, 1987) and orientation, water chemistry, loading frequency separately and synergistically (Van Der Sluys, 1985, 1987；Amzallag, 1983；O'Donnell, 1995；Eason, 1993；Roth, 2003；Chopra, 1998；Atkinson, 1986；Shoji, 1986). The sulfur content has been reported to enhance the corrosion fatigue crack growth rates of low alloy steels (Tice, 1986). Hydrogen water chemistry (HWC) has proved to be a powerful method for mitigating environmentally-assisted cracking (EAC) of stainless steel and nickel-base alloy components. Ritter (Ritter & Seifert, 2007) demonstrated HWC resulted in a significant drop in low-frequency corrosion fatigue crack growth rates by at least one order of magnitude with respect to normal water chemistry (NWC) conditions for pressure vessel steels with sulfur content lower than 0.02 wt %. It is of practical and academic interest to study the effect of HWC on the mitigation of corrosion fatigue initiation and propagation for low alloy steels. The slip-oxidation mechanism has been widely accepted to account for the crack propagation of the carbon and low alloy steels in LWR water systems (Ford, 1987). This mechanism relates crack advance to the oxidation rate that occurs at the crack tip. In order to better predict the crack growth rates of low alloy steels, the interaction between the oxide films and sulfur ion dissolved from steels in the oxygenated or HWC water environments should be clarified.

In this study, the low cycle fatigue and corrosion fatigue crack growth tests were performed on A533B3 low alloy steels with different sulfur contents under simulated BWR coolant

conditions. Corrosion fatigue tests were conducted in different water chemistry including air saturated, deoxygenated by nitrogen and hydrogen. The fracture features of fatigued specimens were studied with optical stereography and scanning electron microscopy (SEM).

2. Experimental procedures

2.1 Materials

A533B3 steel plates with three sulfur content levels ranging from 0.008 wt % (weight percent) to 0.027 wt % were manufactured according to the specifications of ASTM A533. The materials were rolled from a thickness of 150 mm to 30 mm and solution treated at 900℃ for 1.5 hours, then quenched and tempered at 670℃ for 1.5 hours. Their chemical compositions and mechanical properties are given in Tables 1-2, respectively.

Designation	Composition (wt%)									
	C	Si	Mn	P	S	Ni	Mo	A1	N	Fe
Y1	0.19	0.22	1.22	0.015	0.008	0.60	0.49	0.035	0.005	Bal.
Y2	0.19	0.22	1.27	0.015	0.016	0.60	0.49	0.035	0.005	Bal.
Y3	0.21	0.23	1.25	0.015	0.027	0.60	0.49	0.035	0.005	Bal.

Solution treated at 900ºC for 1.5 hour, then quenched and tempered at 670ºC for 1 hour.

Table 1. Chemical compositions of A533B3 steels

Designation	Temperature (℃)	Ultimate tensile strength (MPa)	Yield strength (MPa)	Total elongation (%)	Uniform elongation (%)
Y1	25	711	625	30.3	10.5
	300	692	510	31.1	13.2
Y2	25	686	600	30.6	10.3
	300	680	516	30.1	12.1
Y3	25	722	630	28.6	10.1
	300	722	550	31.2	13.2

Table 2. Mechanical properties of A533B3 steels

2.2 Metallographic examination

To reveal the MnS morphology and carbide/nitride precipitate distribution of the low alloy steels, the as-received specimens were polished following a standard metallographic practice, then etched in a 5 vol. % Nital solution (5 vol. % nitric acid and 95 vol. % ethanol) for about 20 seconds and examined with optical microscopy.

2.3 Low-cycle fatigue test

According to the ASTM E 606 specifications, round bar fatigue specimens with a gage length of 16 mm and diameter of 8 mm were machined, as shown in Fig. 1. Before fatigue testing, all specimens were well polished as per the recommendations of ASTM E 606. The strain was measured by an LVDT extensometer which was calibrated by a strain gage.
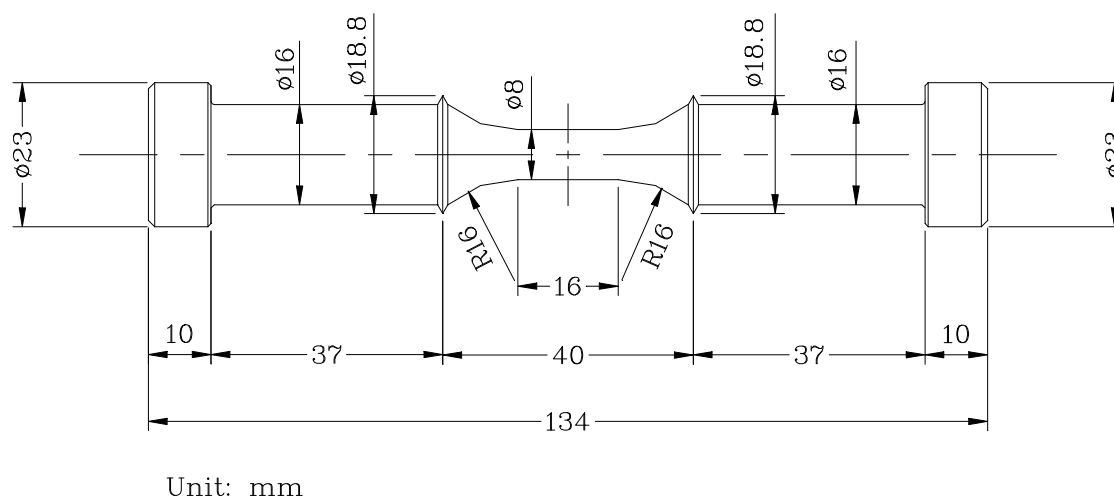
Unit: mm

Fig. 1. Round bar specimen for low-cycle fatigue test.

The low-cycle fatigue tests were conducted on a 100 kN close-loop servo-electric machine under strain control and at a strain rate of 4×10^{-3}/sec. All fatigue tests were performed with a fully reversed axial strain (i.e., strain ratio R = -1) and a triangular waveform in air and water environments, respectively. The strain amplitude was controlled at ±0.1 %, ±0.2 %, ±0.4 %, or ±0.7 %, respectively. The steel specimens were loaded in the rolling direction. Fatigue tests were stopped when specimens broke or the fatigue cycles reached 5×10^5 cycles.

2.4 Fatigue crack growth rate test

According to the ASTM E 647 specifications, compact-tension type (CT) specimens with a thickness of 12.5 mm and a width of 50 mm were machined. Before fatigue testing, all specimens were lightly polished with emery paper to #600. The specimens were pre-cracked by cyclic loading with decreasing ΔK (stress intensity factor range), at a load ratio (R, Pmin/Pmax) of 0.1, till a precracked length of 3 mm and ΔK of 10 MPa $\sqrt{m}$ were reached. In order to have valid test results, the specimen was designed to be predominantly elastic for the applied ΔK values less than 50 MPa $\sqrt{m}$ as per the size requirements of the ASTM E647. The corrosion fatigue tests were conducted on a closed-loop, servo-electric machine with a water circulation loop under constant load amplitude control with a sinusoidal wave form and at the frequencies of 0.02 and 0.001 Hz, respectively. The constant load amplitude was set at an R ratio (Load$_{min}$/Load$_{max}$) of 0.2 by an inner load cell control, which deducted the friction force between the pulling rod and the sealing material. The external load cell measurements including the friction force were also monitored for a comparison with the ones taken by the inner load cell. The electrochemical corrosion potential (ECP) was measured with Ag/AgCl/0.1 M KCl reference electrode. The conditions of the water environment are summarized in Table 3. The crack length was measured by an alternative current potential drop (ACPD) technique. The final fatigue crack length measurement was further calibrated against the average value of five measurements taken along the crack front on the fracture surface by a microscope at a magnification of 20 according to ASTM E

647. After corrosion fatigue tests, the oxide layers on the fracture surfaces were descaled with an electrolyte of 2 g hexamethylene tetramine in 1000 cm³ of 1N HCl (Chopra, 1998) and further investigated with scanning electron microscopy.

Test parameters	Air-saturated (with filtered air)	Deoxygenated (with nitrogen)	HWC
Pressure, MPa	10	10	10
Temperature, ℃	300	300	300
Conductivity(inlet), μScm^{-1}	0.8	0.08	0.065
Conductivity(outlet), μScm^{-1}	1.2	0.16	0.072
Hydrogen(inlet),	N.A.	N.A.	48 ppb
Hydrogen(outlet),	N.A.	N.A.	39 ppb
Oxygen(inlet),	7.4 ppm	1~10 ppb	1~10 ppb
Oxygen(outlet),	6.7 ppm	1~10 ppb	1~10 ppb
ECP(SHE)	0.2 volt	-0.55volt	-0.6 volt
pH(inlet)	5.95	6.88	6.58
pH(outlet)	6.17	6.74	6.76
Autoclave exchange rate	1 time/h	1 time/h	1 time/h

Table 3. Test conditions of high-temperature water environments
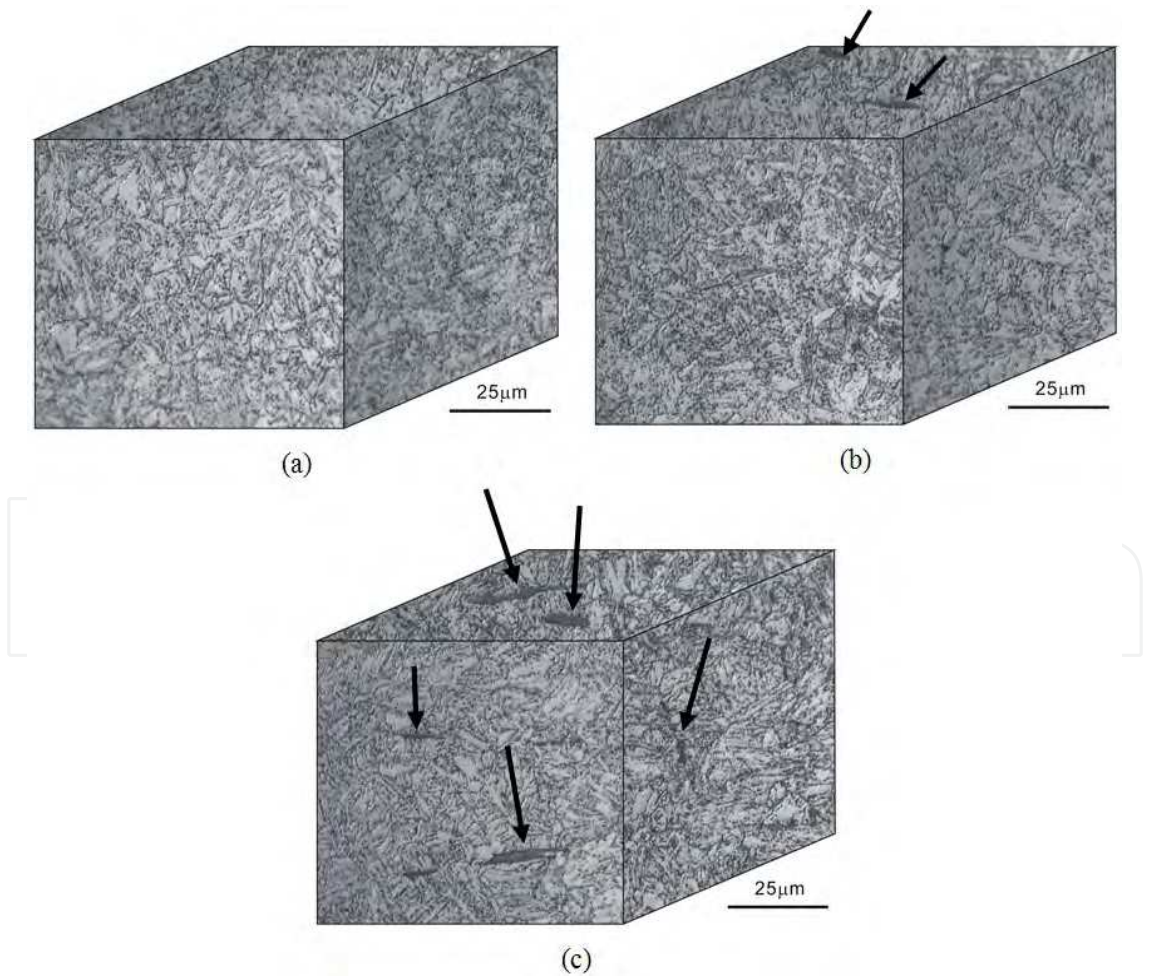
Fig. 2. Metallographs of A533B3 steels with different sulfur contents, (a) 0.008 wt%, (b) 0.016 wt%, (c) 0.027 wt%. (The arrows indicate the sulfides.)

3. Results and discussion

3.1 Metallographic examination

The metallographs of A533B3 steels with different sulfur contents are shown in Fig. 2. The sulfide laths were identified by energy dispersive spectroscopy (EDS) and observed to be oriented in the rolling direction for A533B3 steels. Little or no sulfides were observed for the steel with the lowest sulfur content. Tempered martensite was prevalent in the steels.

3.2 Low cycle fatigue life

The low-cycle fatigue lives of the steel specimen with 0.016 wt% sulfur under different environments are shown in Fig. 3. The fatigue life was significantly affected by the test temperature, strain amplitude, and oxygen level in the water environment. Regarding the environment effect, the steel specimens showed the shortest fatigue life in the air saturated water environment and the longest life in air at 300°C. The fatigue life with the lower oxygen level in the water environment showed the longer fatigue life. At the strain amplitude of ±0.2 %, the steel specimens tested in air had a much longer fatigue life at 300°C than at room temperature. This could be accounted for by the occurrence of dynamic strain aging and the effect of grain size reduction at 300°C (Huang, 2003, 2004). Lee and Kang (Lee, 1995 ; Kang, 1992) demonstrated that dynamic strain aging would improve the low-cycle fatigue resistance and degrade the fracture toughness at 300°C for the pressure vessel steel SA508 class 3 in air. It is consistent with the results of this study that a higher fatigue life was observed at 300°C than at room temperature in air.

The temperature effect on the fatigue life at a strain amplitude of ±0.4 % in the air saturated water environment and air is presented in Fig. 4. The longest fatigue life occurred at 245°C in the both environments. A similar result was reported by Chopra and Shack (Chopra & Shack, 1998) that the steel A333-Gr 6 exhibited the best fatigue resistance at 250°C in air. A large difference in fatigue life between 250°C and 300°C was also noted. The reason that fatigue life was enhanced at 245°C in the air-saturated water environment could be related to the negative strain rate sensitivity in the temperature range from 150℃ to 300℃, as shown in Fig. 5. Nakao et al. (Nakao, 1995) also had a similar inference from a study of A333-6 steel. The effect of temperature on fatigue life in the water environment with 200 ppb oxygen is shown in Fig. 6. At the strain amplitude of ±0.2 % or ±0.4 %, the effect of temperature on fatigue life was not significant in the range from 150°C to 300°C. It could be accounted for by a remarkable reduction in fatigue-corrosion interaction due to the formation of dense oxide film on the specimen thereby extending the steel fatigue life. Consequently the fatigue life showed no much change from 150°C to 300°C under the present water environment. A similar dependence of fatigue life on temperature was also predicted from a statistical model reported by Chopra and Shack (Chopra & Shack, 1998), but they further indicated that the fatigue life would decrease significantly with increasing temperature in the range from 150°C to 300°C when the applied strain rate was reduced to 4×10^{-5} s^{-1}. Fig. 7 illustrates the relationship of the fatigue life against strain amplitude for A533B3 steels with different sulfur contents tested in 300°C water environments with saturated air and hydrogen, respectively. The low-cycle fatigue life of

the steel specimen in the hydrogenated water increased significantly relative to that obtained in the air-saturated water environment. Under the strain rate of $4x10^{-3}s^{-1}$, the fatigue life of the specimen was not varied with its sulfur content in both water environments. This result is consistent with the report of Chopra and Shack (Chopra & Shack, 1998). The data further indicated that the fatigue life of low alloy steel with the sulfur content 0.003 wt% was ten times longer than that with the sulfur content 0.010 wt% when the strain rate was decreased to $4x10^{-6}s^{-1}$. On the contrary, for the steel with the sulfur content higher than 0.012 wt%, the effect of sulfur content on the low cycle fatigue life was insignificant. Their limited data suggested that environmental effects on fatigue life may become saturated for the specimens with sulfur contents higher than 0.012 wt% when the strain rate was controlled at $4x10^{-3}s^{-1}$.
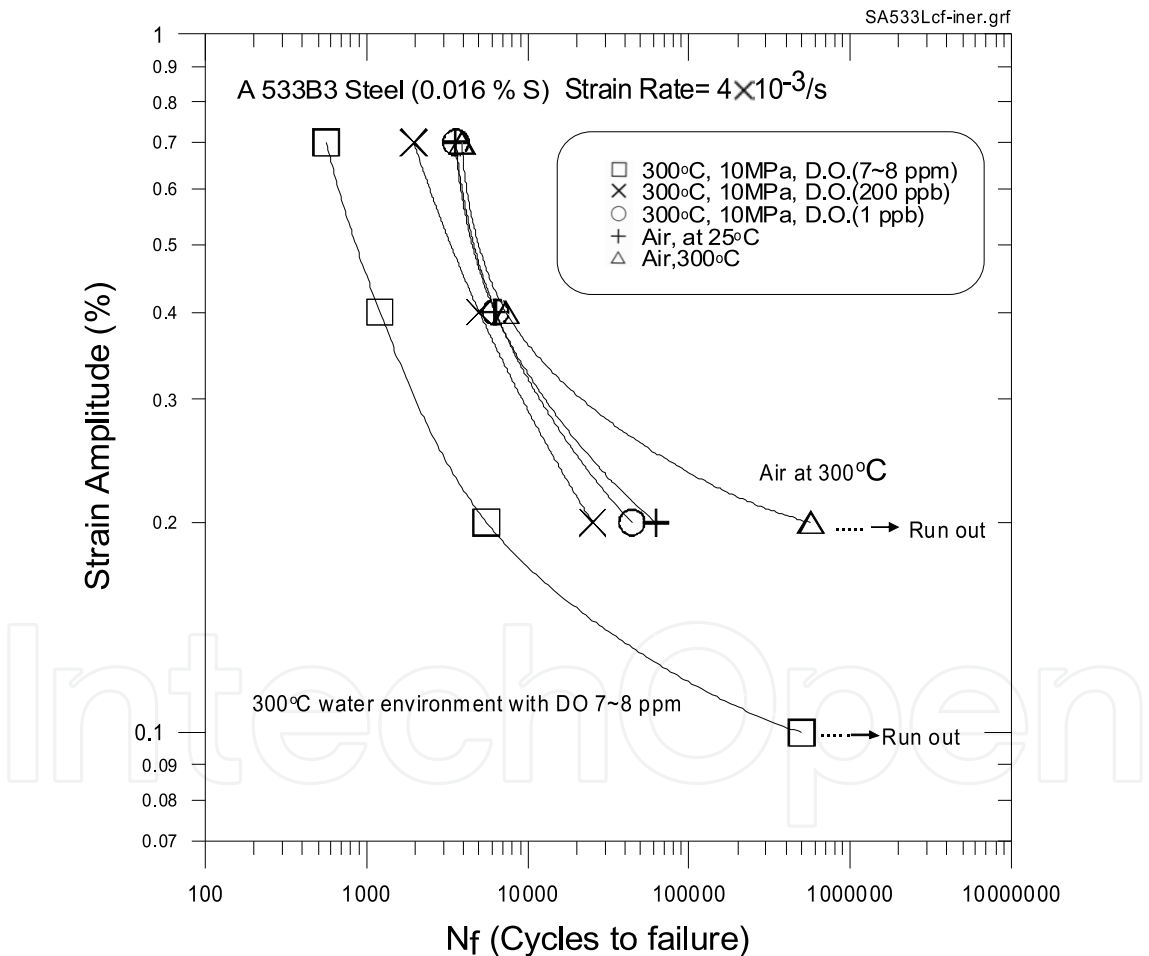
Fig. 3. Relationships between the low-cycle fatigue life and strain amplitude for A533B3 steel with 0.016 wt% sulfur tested in different environments.
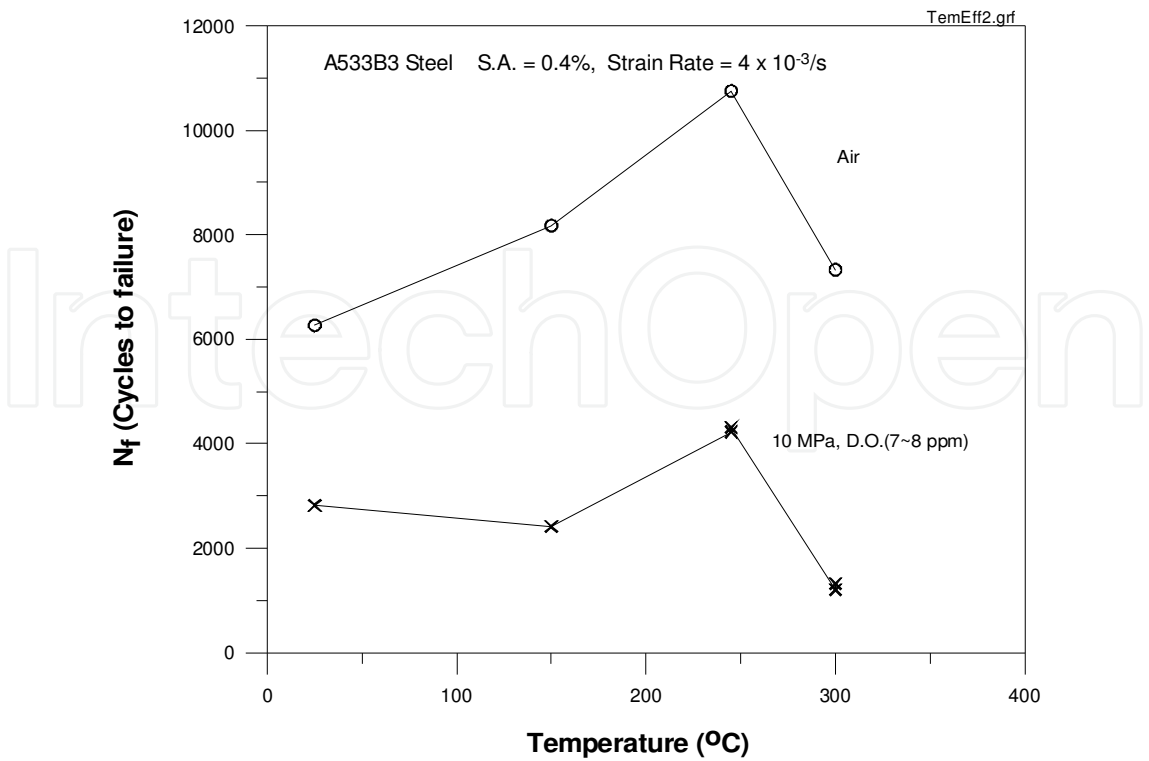
Fig. 4. Effect of temperature on fatigue life of A533B3 steel in the air-saturated water environment and in air.
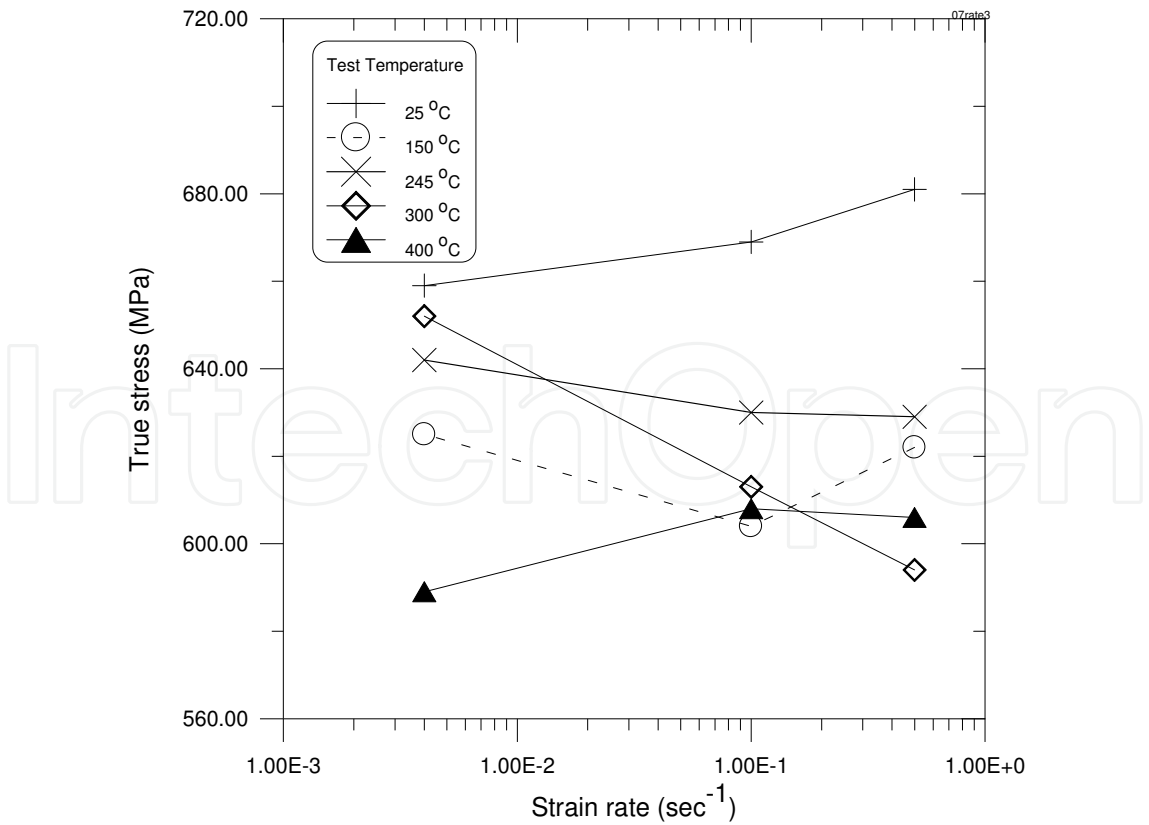

Fig. 5. Effect of strain rate on the true stress of A533B3 steel at a true strain of 2% tested at different temperatures in air.
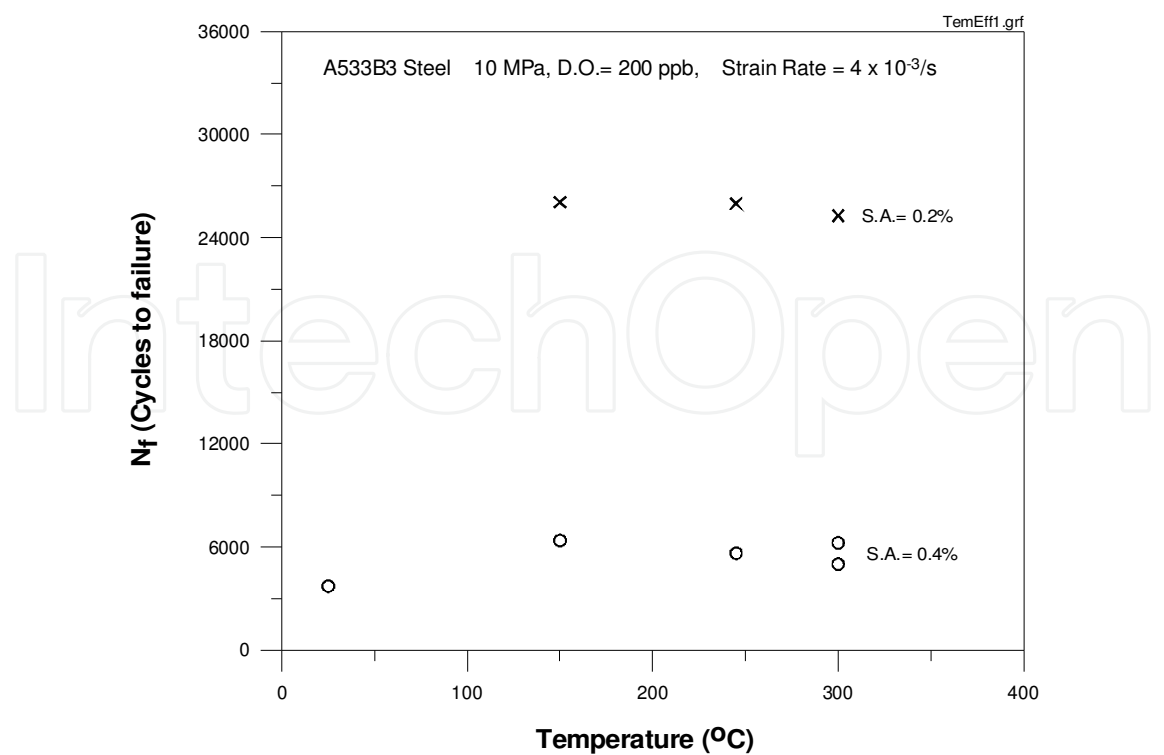
Fig. 6. Effect of temperature on fatigue life of A533B3 steel in the water environment with an oxygen content 200 ppb.
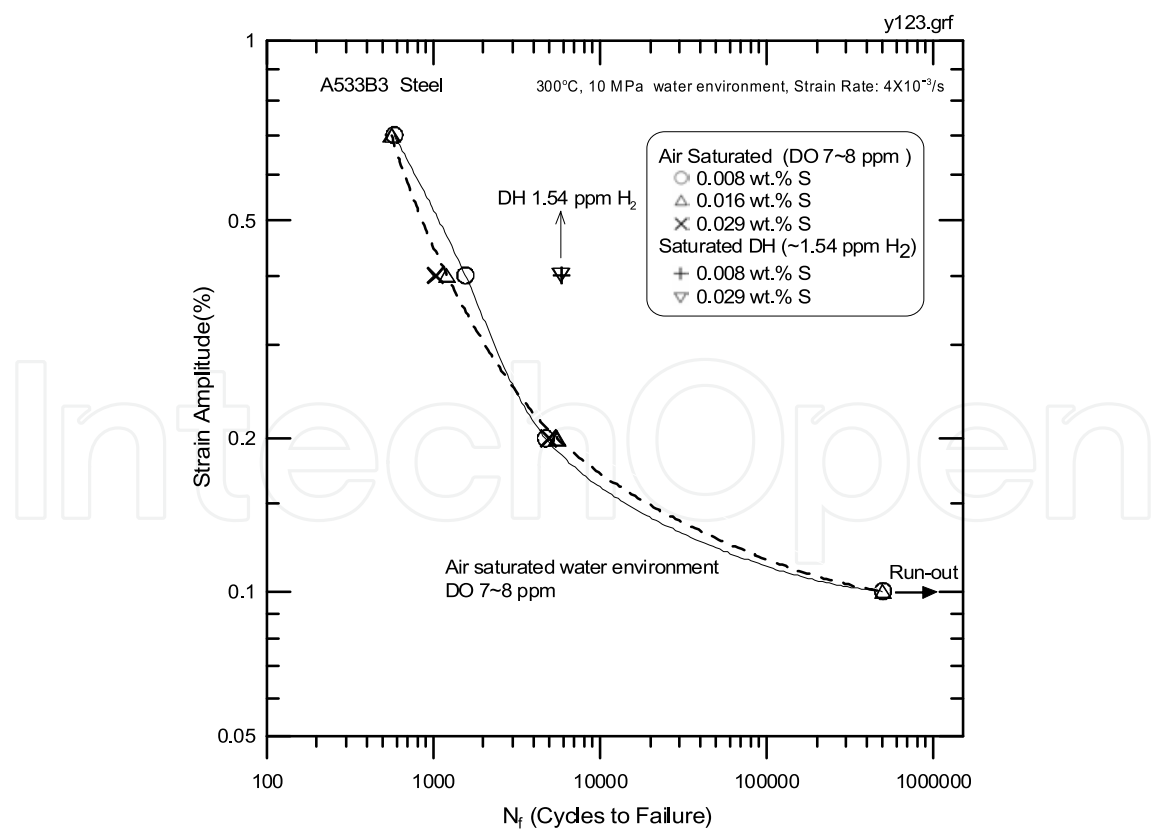

Fig. 7. Relationships between the low-cycle fatigue life and strain amplitude for A533B3 steels with different sulfur contents tested in 300°C water environments .

3.3 Effects of sulfur content on fatigue crack growth rate of low alloy steels

The fatigue crack growth rates of A533B3 steels with three sulfur content levels in water environments at 300℃ are shown in Fig. 8. In the air-saturated water environment, Fig. 8(a), there was no significant difference in the fatigue crack growth rates of the steels with different sulfur contents at a loading frequency of 0.02 Hz. But in the deoxygenated water environment, the lower corrosion fatigue crack growth rate was observed for the steels with lower sulfur contents. For the steel with 0.016 wt% sulfur, the corrosion fatigue crack growth rate increased significantly when the stress intensity factor range was larger than $38MPa\sqrt{m}$, as shown in Fig. 8(b). Fig. 9 presents the results of A533B3 steel tested in an air-saturated water environment at a loading frequency of 0.001 Hz. The data outside the bounds of the ASME XI wet curves are not conservative. It was noted that the fatigue crack growth rates were almost the same for the steels of medium(0.016 wt% sulfur) and high sulfur content (0.027 wt% sulfur), but that those with low sulfur content showed the lowest crack growth rate. From the above results, it can be concluded that the high sulfur in low alloy steels or the high dissolved oxygen in the water coolant or their synergistic effects would degrade the corrosion fatigue resistance of low alloy steels. Therefore, it is essential to secure the integrity of pressure vessel by reducing the steel sulfur content during the steel manufacturing and by decreasing oxygen content in the reactor coolant, for instance, by HWC.
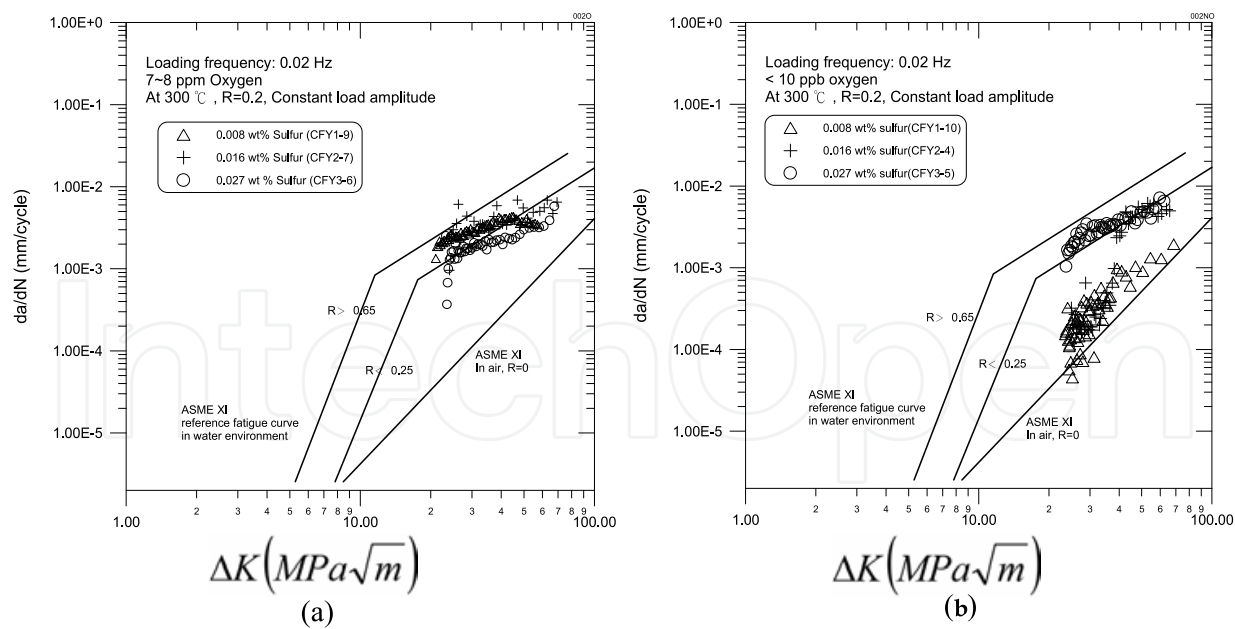

Fig. 8. Sulfur content effects on the corrosion fatigue crack growth rates of A533B3 steels in the water environments of different oxygen contents at a loading frequency of 0.02 Hz: (a) 7~8 ppm oxygen and (b) ＜10 ppb oxygen.
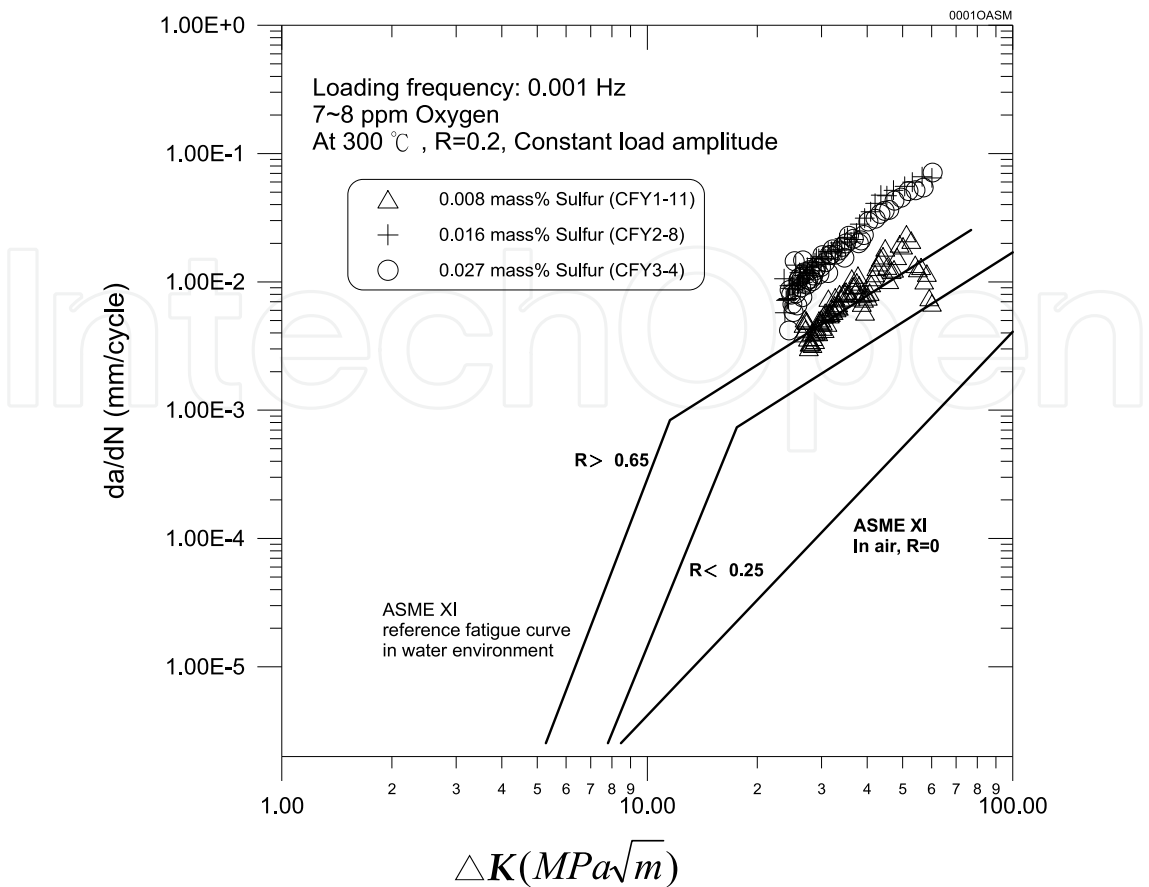
Fig. 9. Sulfur content effects on the corrosion fatigue crack growth rates of A533B3 steels in an oxygen saturated water environment at a loading frequency of 0.001 Hz.

3.4 Water chemistry effects on fatigue crack growth rate

Fig. 10 makes a comparison of fatigue crack growth rates for A533B3 steels with three sulfur levels tested in the deoxygenated and air-saturated water environments. It is clear that an increase in oxygen level accelerates crack growth in the steel specimens with sulfur contents up to 0.016 wt %. For the steel with 0.027 wt% sulfur, the opposite is true. Their corrosion fatigue crack growth rates are faster in the water environment with near zero dissolved oxygen concentration than with 7~8 ppm dissolved oxygen concentration, as shown in Fig. 10(c). Figure 11 shows a comparison of fatigue crack growth rates for the high sulfur steels tested in the high temperature water environments deoxygenated by nitrogen and hydrogen, respectively. The fatigue crack growth rate is in good agreement with each other. Both curves show a surged crack growth rate phenomenon, similar to Fig. 10(b). In Fig. 10(b), for the steel specimens with 0.016 wt% sulfur content, the fatigue crack growth rate in the deoxygenated water environment surged to the same levels as those tested in the air saturated water environment when the concentration of sulfate ion reached a critical concentration in the crack tip. A surge of the fatigue crack growth rate occurred, when the applied $\triangle$K reached a value of ~35 MPa $\sqrt{m}$. Correspondently, a pseudo boundary was identified on the fracture surface of the specimen, as shown in Fig. 12(a). The boundary was further examined by SEM at higher magnifications to consist of a band of microcracks, which is a unique feature not observed in other regions, as shown in Figs. 12(b) and (c).
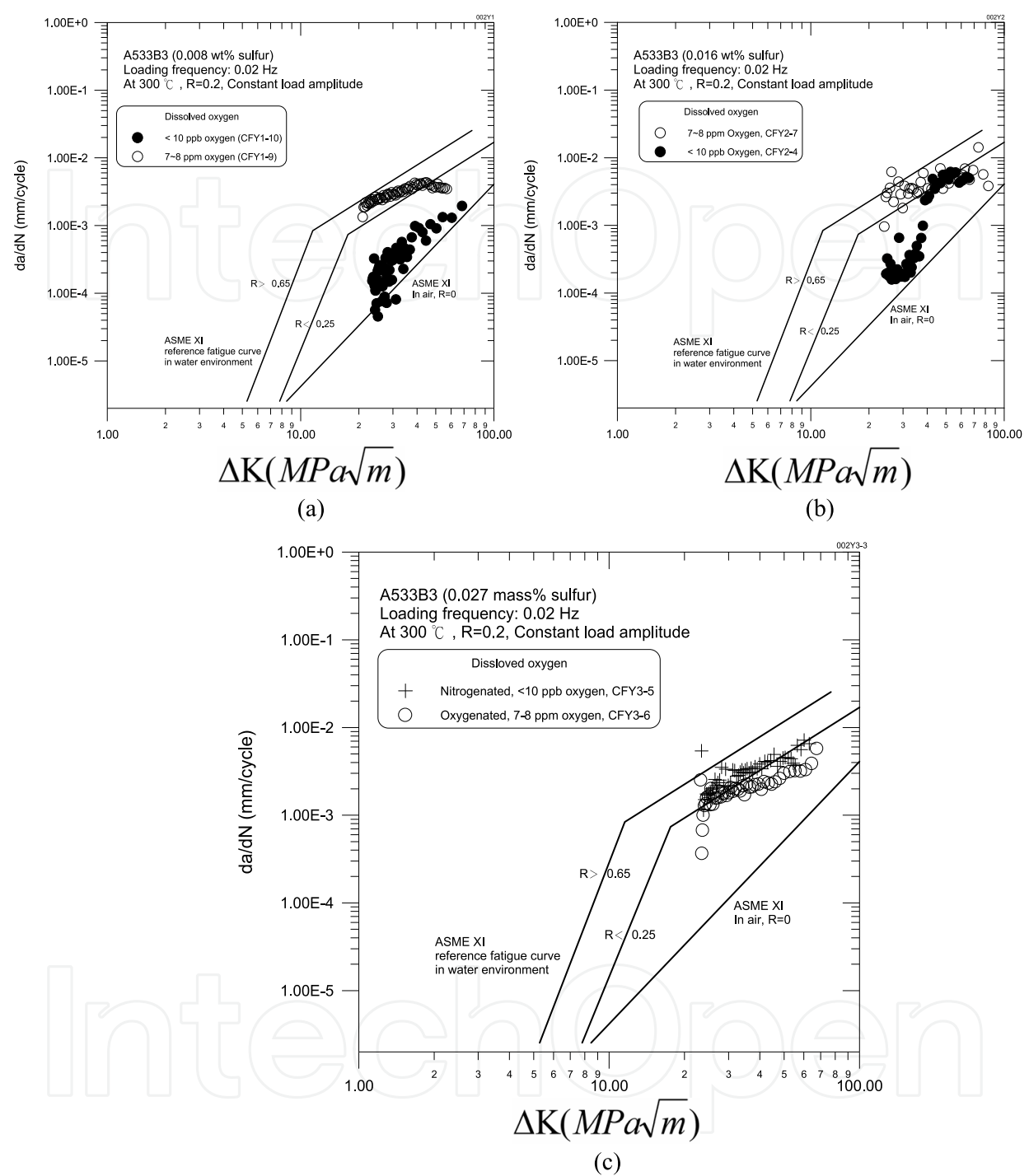
Fig. 10. A comparison of fatigue crack growth rates for A533B3 steels tested in high temperature deoxygenated and air-saturated water environments, (a) steel sulfur content 0.008 wt%, (b) steel sulfur content 0.016 wt%, and (c) steel sulfur content 0.027 wt%.

There were some inclusions imbedded in the microcracks. The inclusions containing sulfides were identified by EDS. The surged fatigue crack growth rate and a pseudo boundary were also observed with the 0.027 wt % sulfur specimens in the deoxygenated water environment, as indicated in Fig. 11. The probabilities of finding a surged fatigue crack growth rate were

strongly related to the specimen sulfur levels. The greater the sulfur level, the greater the probability to find a surged growth rate. It implies the sulfides dissolved in the coolant environment around the crack tip may speed up the crack growth rate when sulfur ion reached a critical quantity. A previous study (Yeh, 2007) showed that the dense oxide film, Fe_3O_4, was formed when low alloy steel specimens were tested in the deoxygenated water environments at 300℃. The corrosion products in a 10 MPa water environment with saturated air at the test temperature 300℃ were identified to be a porous mixture of Hematite (α-Fe_2O_3) and Maghemite (γ-Fe_2O_3). The porous oxide layer allows the coolant water access to the fresh metal beneath it and provides less protection than the dense one does. As a result, there was a relatively larger proportion of fresh metal with the porous oxide layers on the specimens than those with dense ones exposed to the coolant, as illustrated in Fig. 13. A hypothesis is proposed to elucidate the observation under the assumptions that sulfate ions have higher affinity to fresh metal than to the oxide layer and that the quantities of sulfate dissolved from specimens in the air saturated and deoxygenated water environments are comparable. The sulfate ion in the coolant will transport to the fresh surface around the crack tip and the fresh metal beneath the porous oxide layer. In relative terms, there was less fresh metal surface of the specimen exposed to the deoxygenated water coolant than to the air-saturated one. The concentration of sulfate ion in the coolant in front of the crack tip of the specimens with dense oxide layer would be relatively higher than that with porous oxide layer. The attack of sulfate ions on the crack tip of the specimens tested in deoxygenated water environment would be more aggressive than those tested in air saturated water environment when sulfate ions reached a critical concentration. The sulfur dissolved in the high temperature water environment from the high-sulfur steels was sufficient to acidify the crack tip chemistry. Therefore, the deoxygenated water environment showed little or no beneficial effect for the high sulfur steels. To mitigate the environmentally assisted cracking of low alloy steels, the factor of sulfate ion in the coolant should be taken into account.
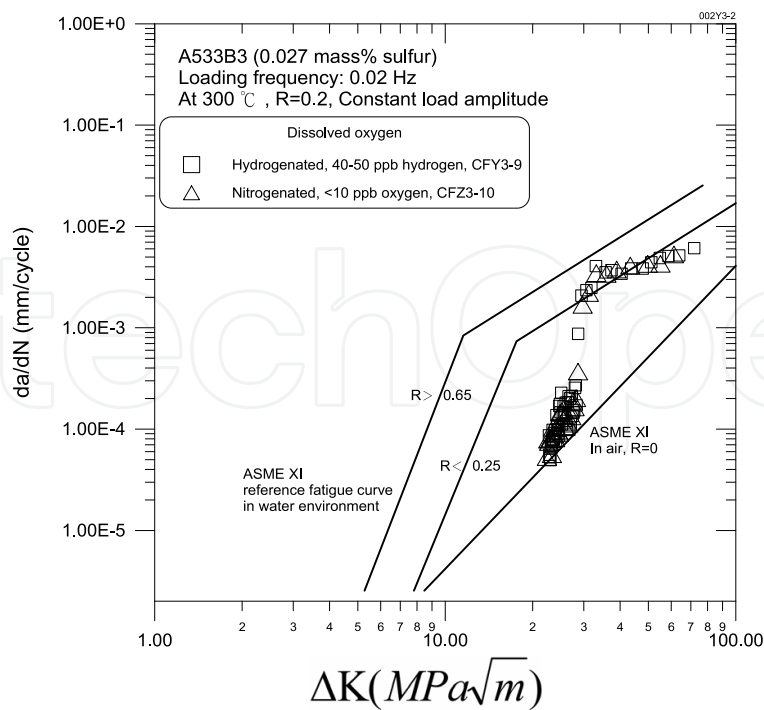

Fig. 11. A comparison of fatigue crack growth rates for A533B3 steels tested in high temperature water environments deoxygenated by nitrogen and hydrogen, respectively.
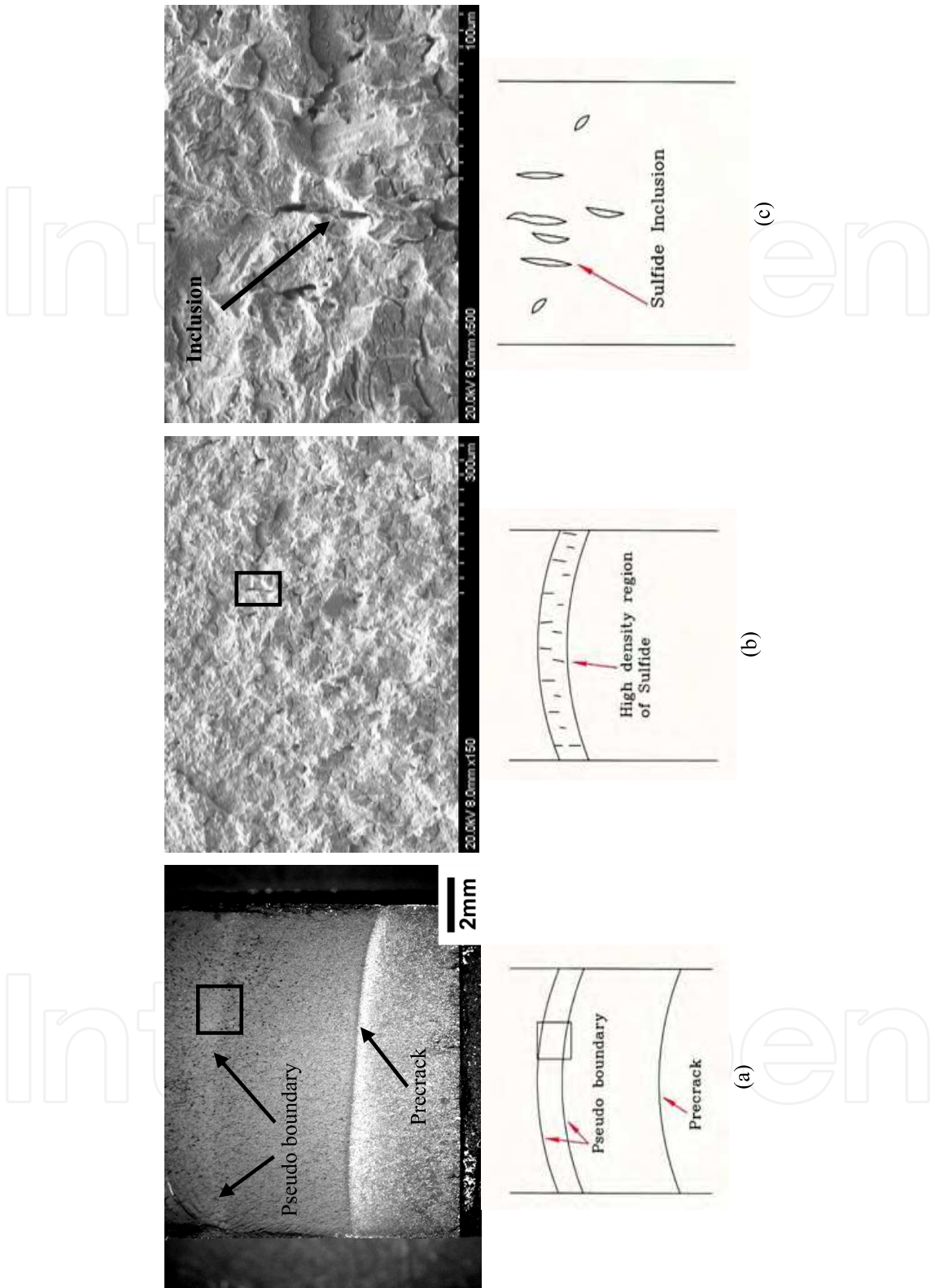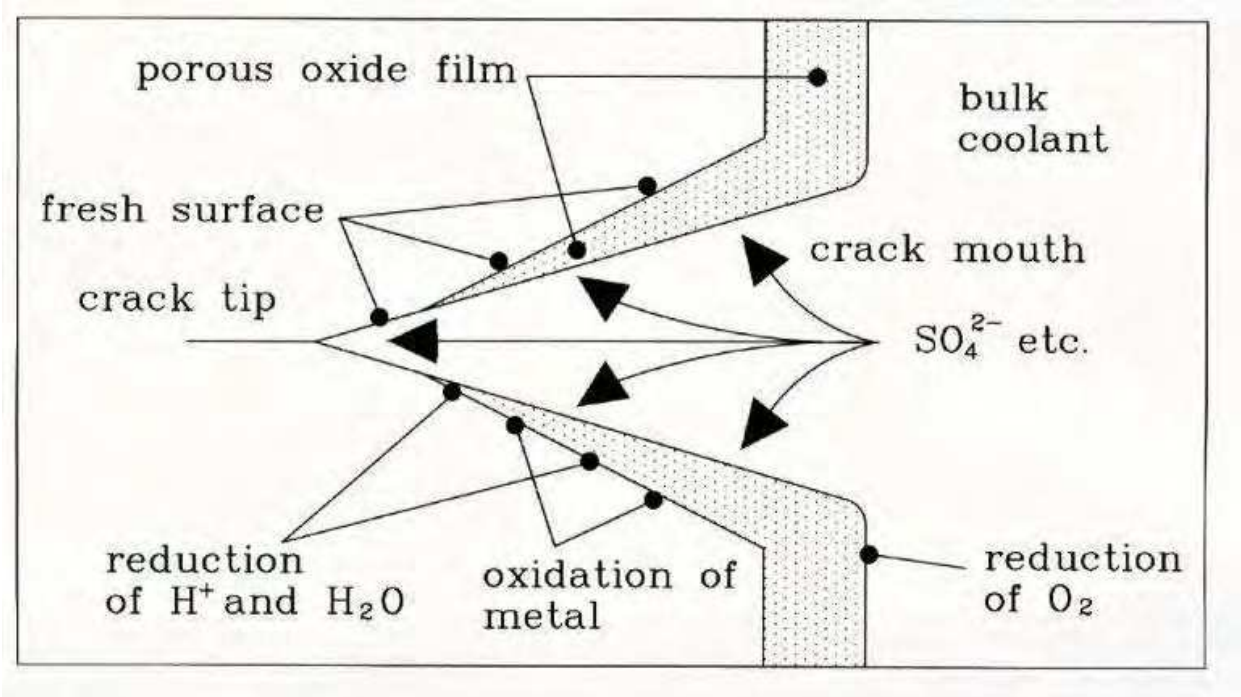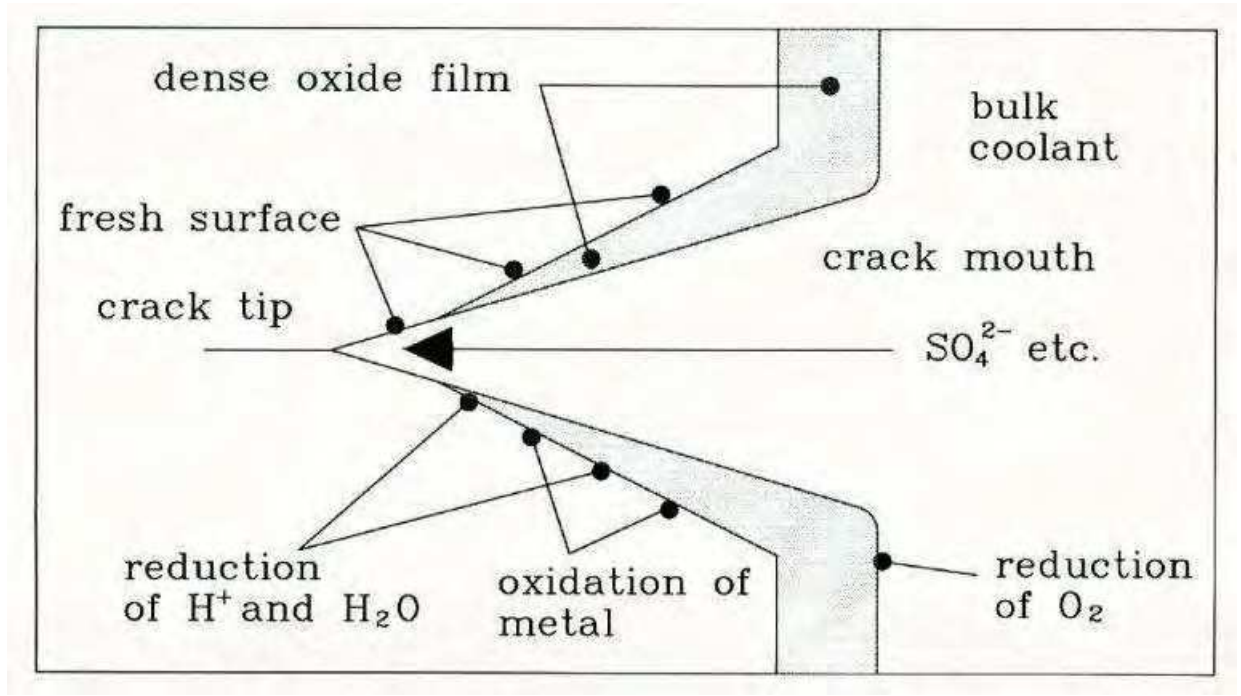
Fig. 12. A pseudo boundary observed on the fracture surface of the steel specimen with sulfur content 0.016 wt % tested at a loading frequency of 0.02 Hz in deoxygenated water environment, (a) fractographic feature by optical stereography, (b) a band of microcracks boxed up in (a) examined by SEM, (c) microcracks boxed up in (b) at a higher magnification.

(a)

(b)

Fig. 13. A schematic illustration of (a) porous oxide film formed in an oxygenated water environment and (b) dense oxide film formed in a deoxygenated water environment.

3.5 Frequency effects on fatigue crack growth rate

Fig. 14 illustrates the frequency effects on the fatigue crack growth rate of A533B3 steels in the air saturated water environment. The lower the frequency, the higher the fatigue crack growth rate was observed for all the three steel specimens with different sulfur levels.
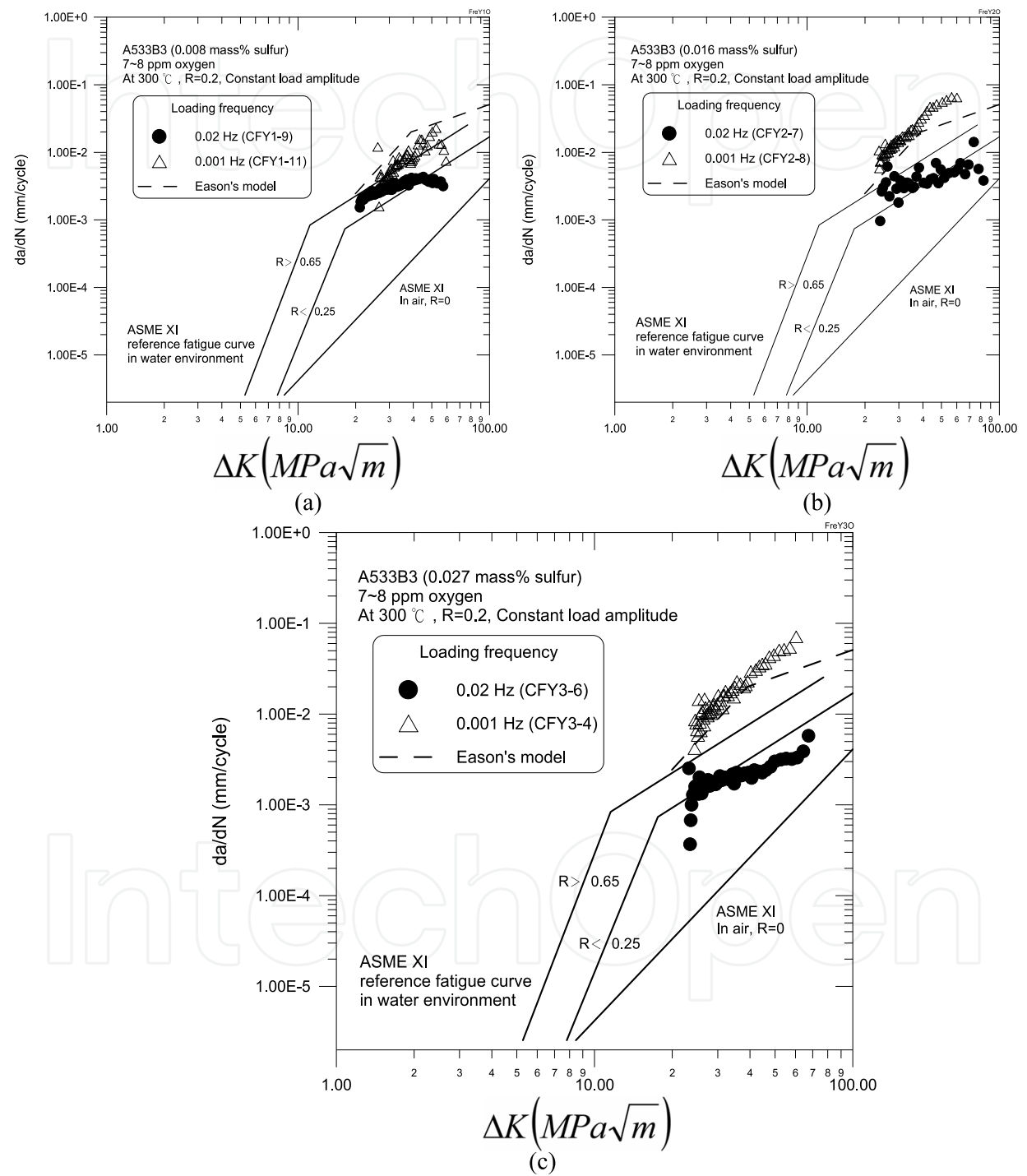

Fig. 14. Frequency effects on corrosion fatigue crack growth rates for A533B3 steels with different sulfur levels tested in 300℃ air-saturated water environment: (a) 0.008 wt% S, (b) 0.016 wt% S, and (c) 0.027 wt % S.

It means that the corrosion fatigue resistance of A533B3 steels was significantly affected by the loading frequency in the air-saturated water environment. In the GE-model (Ford, 1987) the corrosion fatigue (CF) crack growth through anodic dissolution is controlled by the crack-tip strain rate and the sulfur anion activity/pH in the crack tip electrolyte that govern the oxide film rupture and the dissolution/repassivation behavior after the film rupture event. From Fig. 13, the data points not bounded by the Eason's model (Eason, 1998) were attributed to the factors of the low frequency and higher sulfur content as well as high dissolved oxygen in the water coolant. These results are different from the observation that the initiation life is significantly decreased when the applied strain range, temperature, DO level in water, sulfur content in steel and strain rate are simultaneously satisfied. One individual factor will enhance the crack growth rates when it is higher than their threshold. Therefore, it is inferred that the benefit factors for the crack initiation are also beneficial for the crack growth of low alloy steels.

(a)   (b)
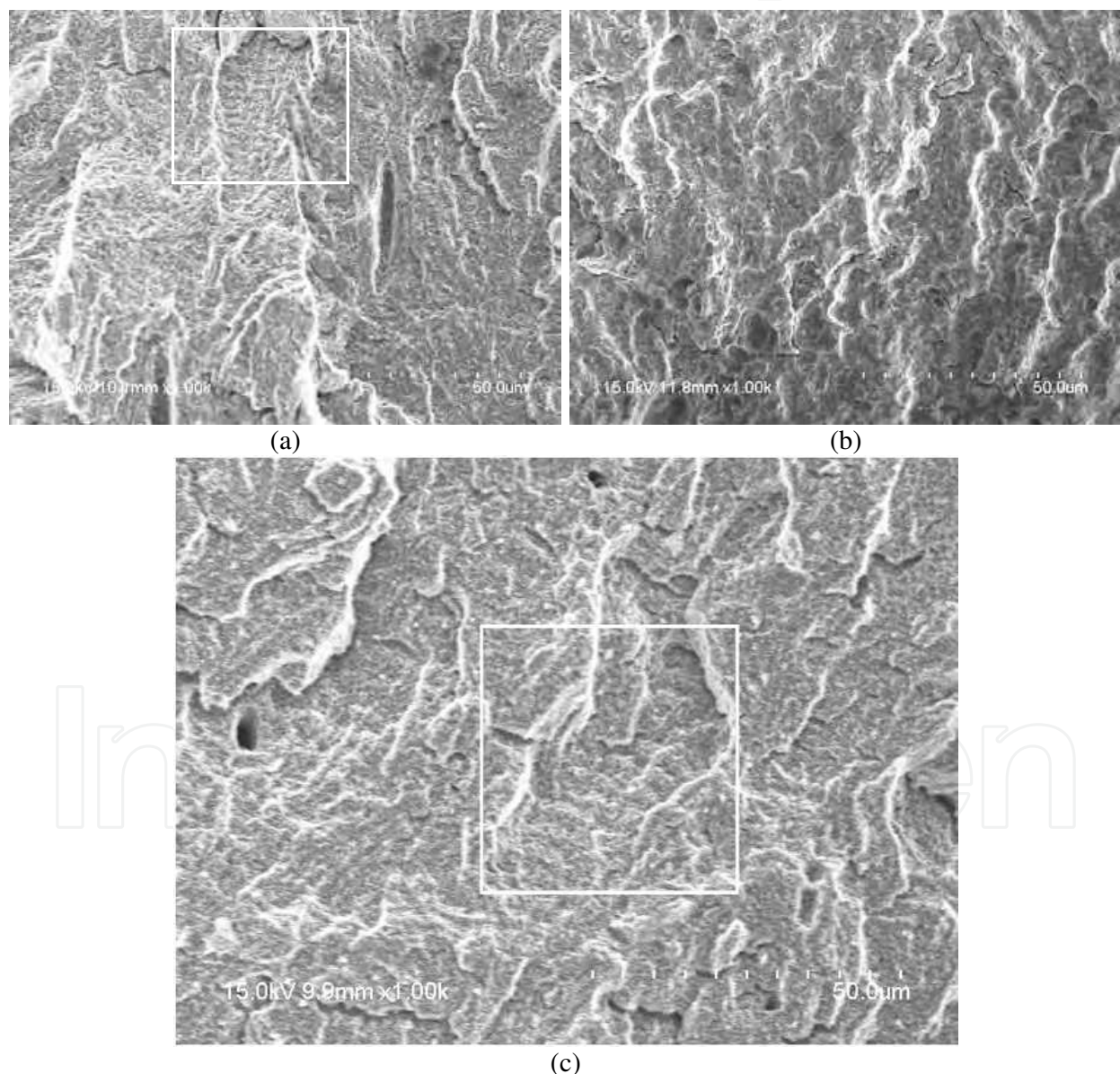
(c)

Fig. 15. SEM fractographs for A533B3 steel specimens with sulfur content 0.016 wt % tested in high-temperature water environments: (a) 0.02 Hz, air-saturated (b) 0.001 Hz, air-saturated, (c) 0.001 Hz, deoxygenated.

Distinct fracture features were revealed by SEM for the fatigue specimens tested in the high-temperature water environments at different frequencies. The fracture features were apparently related to the oxidation behavior. For the tests at a loading frequency of 0.02 Hz in the air-saturated water environment, the specimen revealed fatigue striation pattern, as shown in Fig. 15(a). The striations could have been corroded due to a long stay at a loading frequency of 0.001 Hz in an air-saturated water environment, illustrated in Fig. 15(b). By contrast, the striations were manifested in the deoxygenated water environment at a loading frequency of 0.001 Hz, as shown in Fig. 15(c).

4. Conclusions

1. The low cycle corrosion fatigue results show that a significant temperature effect on the fatigue life was observed for the specimen tested in the oxygenated water environment at the temperature range from 150℃ to 300℃, but little or no dependence of fatigue life on temperature was noted in the deaerated water environment with an oxygen content 200 ppb.
2. Under the strain rate of $4 \times 10^{-3} s^{-1}$, the fatigue life of the specimen was not varied with its sulfur content in the air saturated and hydrogenated water environments.
3. Corrosion fatigue crack growth rates of A533B3 steels were significantly affected by the steel sulfur content, loading frequency and oxygen content in the high-temperature water environment. The data points outside the bound of Eason's model could be attributed to the low frequency, higher sulfur content and high dissolved oxygen water coolant.
4. The sulfur dissolved in the water environment from the higher sulfur steels was sufficiently concentrated to acidify the crack tip chemistry even in the HWC water. Therefore, nitrogenated or HWC water did not show any beneficiary effect on the high-sulfur steels.

5. Acknowledgments

6. References

Shah, V. N. & Macdonald, P. E. (1993). *Aging and Life Extension of Major Light Water Reactor Components*, Amsterdam, Elsevier Science Publishers.

Huang, J. Y., Li, R. Z., Chien, K. F., Kuo, R. C., Liaw, P. K., Yang, B. & Huang, J. G. (2001), Fatigue behavior of SA533-B1 steels, in: *Fatigue and Fracture Mechanics, 32nd vol., ASTM STP 1406*, R. Chona (Ed.), Philadelphia, PA, pp. 105-121.

Huang, J. Y.；Chen, C. Y.；Chien, K. F.；Kuo, R. C.; Liaw, P. K. & Huang, J. G., in: *Proc. Julia Weertman Symp., TMS Fall Meeting*, Oct. 31- Nov. 4, 1999, pp. 373-384.

Seifert, H. P.；Ritter, S. & Heldt, J. (2001), Strain induced Corrosion Cracking of Low-alloy Reactor Pressure Vessel Steels under BWR Conditions, in: F. P. Ford, G. S. Was

and J. L. Nelson (Eds.), *Proceedings of the 10th International Conference on Environmental Degradation of Materials in Nuclear Power System-water Reactors*.

Seifert, H. P.; Ritter, S. & Hickling, J. (2003), Environmentally-assisted Cracking of Low-alloy RPV and Piping Steels under LWR Conditions, in: G. S. Was, L. Nelson, and P. King (Eds.), *Proceedings of the 11th International Conference on Environmental Degradation of Materials in Nuclear Power System-water Reactors*, pp. 73-89.

Huang, J. Y.; Young, M. C.; Jeng, S. L.; Yeh, J. J.; Huang, J. S. & Kuo, R. C. (2007), Corrosion Fatigue Behavior of an Alloy 52-A508 Weldment under Simulated BWR Coolant Conditions, in: P. King, T. Allen, J. Busby (Eds.), *13th International Conference on Environmental Degradation of Materials in Nuclear Power System*, Whistler, Canada, August 19-23.

Chopra, O. K. & Shack, W. J. (1997), Evaluation of Effects of LWR Coolant Environments on Fatigue Life of Carbon and Low–alloy Steels, in : *Effects of the Environment on the Initiation of Crack Growth*, W. A. V. D Sluys, R. S. Piascik & R. Zawierucha, (Eds), ASTM STP 1298, pp. 247-266.

Huang, J. Y.; Hwang, J. R.; Yeh, J. J.; Kuo, R. C. & Chen, C. Y. (2003), Low Cycle Fatigue Resistance of SA533 Steels, *Mater. Sci. and Tech*. 19, pp. 1575-1584.

Huang, J. Y.; Hwang, J. R.; Yeh, J. J.; Chen, C. Y.; Kuo, R. C. & Huang, J. G. (2004), Dynamic Strain Aging and Grain Size Reduction Effects on the Fatigue Resistance of SA533B3 Steels, *J. Nucl. Mater*. 324, pp. 140-151.

Van Der Sluys, W. A. & Emanuels, R. H. (1985), The Effect of Sulfur Content on the Crack Growth Rate of Pressure Vessel Steels in LWR Environments, in: J. T. A. Roberts (Eds.), *Proceedings of the 2nd International Symposium on Environmental Degradation of Materials in Nuclear Power Systems-water Reactors*, Monterrey, California, September, pp. 100-107.

Amzallag, C.; Bernard, J. L. & Slama, G. (1983), Effect of Loading and Metallurgical Parameters on the Fatigue Crack Growth Rates of Pressure Vessel Steels in Pressurized Water Reactor Environment, in: J. T. A. Roberts (Eds.), *Proceedings of the International Symposium on Environmental Degradation of Materials in Nuclear Power Systems-water Reactors*, Myrtle Beach, South Carolina, August, pp. 727-745.

Combrade, P.; Foucault, M. & Slama, G. (1987), Effect of Sulfur on the Fatigue Crack Growth Rates of Pressure Vessel Steel Exposed to PWR Coolant: Preliminary Model for Prediction of the Transitions between High and Low Crack Growth Rates, in: G. J. Theus. And J. R. Weeks (Eds.), *Proceedings of the Third International Conference on Environmental Degradation of Materials in Nuclear Power System-water Reactors*, pp. 269-276.

Van Der Sluys, W. A. & Cullen, W. H. (1987), Fatigue Crack Growth of Pressure Vessel Materials in Light-water-reactor Environments, in: R. Rungta, J. D. Gilman, and W. H. Bamford (Eds.) *Performance and Evaluation of Light Water Reactor Pressure Vessels*, PVP-119, San Diego, CA., ASME, p. 63-71.

O'Donnell, T. P. & O'Donnell, W. J. (1995), Cyclic Rate-dependent Fatigue Life in Reactor Water, in: S. Yukawa (Eds.), *Performance and Evaluation of Light Water Reactor Pressure Vessels*, PVP-306, Honolulu Hawaii, ASME, July, pp. 59-69.

Eason, E. D. & Nelson, E. E. (1993), Analysis of Fatigue Crack Growth Rate Data for A508 and A533 Steels in LWR Environments, *EPRI TR-102793, Project 2006-20 Final Report, August.*

Roth, A.; Hänninen, H.; Brümmer, G.; Wachter, Ilg, U.; Widern, M. & Hoffmann, H. (2003), Investigation of Dynamic Strain Aging Effects of Low Alloy Steels and Their Possible Relevance for Environmentally Assisted Cracking in Oxygenated High-temperature Water, in: G. S. Was, L. Nelson, and P. King (Eds.), *Proceedings of the 11th International Conference on Environmental Degradation of Materials in Nuclear Power System-water Reactors*, pp. 317-329.

Chopra, O. K. & Shack, W. J. (1998), *Effects of LWR Coolant Environments on Fatigue Design Curves of Carbon and Low-alloy Steels*, NUREG/CR-6583, ANL-97/18, US Nuclear Regulation Commission.

Atkinson, J. D. & Forrest, J. E. (1986), The Role of MnS Inclusions in the Development of Environmentally Assisted Cracking of Nuclear Reactor Pressure Vessel Steels, in: W. H. Cullen (Eds.), *Proceedings of the Second International Atomic Energy Agency Specialist's Meeting on Subcritical Crack Growth*, Sendai Japan, NUREG/CP-0067, US Nuclear Regulation Commission, Vol. 2, pp. 153-178.

Shoji, T.; Komai, K.; Abe, S. & Nakajima, H. (1986), Mechanistic Understanding of Environmentally Assisted Cracking of RPV Steels in LWR Primary Coolants, in: W. H. Cullen (Eds.), *Proceedings of the Second International Atomic Energy Agency Specialist's Meeting on Subcritical Crack Growth*, Sendai Japan, NUREG/CP-0067, US Nuclear Regulation Commission, Vol. 2, pp. 99-117.

Tice, D. R. (1986), Influence of Mechanical and Environmental Variables on Crack Growth in PWR Pressure Vessel Steels, *Int. J. Pres. Ves. and Piping*, 24, pp. 139-173.

Ritter, S. & Seifert, H. P. (2007), Evaluation of the Mitigation Effect of Hydrogen Water Chemistry in BWRs on the Low-frequency Corrosion Fatigue Crack Growth in Low-alloy Steels, *J. Nucl. Mater.*, 360, pp. 170-176.

Ford, F. P.; Taylor, D. E. & Andresen, P. L. (1987), *Corrosion-assisted Cracking of Stainless and Low-alloy Steels in LWR Environments*, EPRI NP-5064M.

Standard Recommended Practice for Constant-amplitude Low-cycle Fatigue Testing (1997), *ASTM E606-80*, pp. 629-641.

Lee, B. H. & Kim, I. S. (1995), *J. Nucl. Mater.*, pp. 226 216.

Kang, S. S. & Kim, I. S. (1992), *Nucl. Technol.* 97, pp. 336-343.

Chopra, O. K. & Shack, W. J. (1998), *Effects of LWR Coolant Environments on Fatigue Design Curves of Carbon and Low-alloy Steels*, Report NUREG/CR-6583, ANL-97/18, pp. 47-52.

Nakao, G.; Kanasaki, H.; Higuchi, M.; Iida, K. & Asada, Y. (1995), Environmental Effects, Modeling Studies, and Design Considerations, American Society of Mechanical Engineers, in: *Fatigue and Crack Growth,* S. Yukawa (ed.),: New York, PVP Vol. 306, pp.123-128.

Yeh, J. J.; Huang, J. Y. & Kuo, R. C. (2007), Temperature Effects on Low-cycle Fatigue Behavior of SA533B Steel in Simulated Reactor Coolant Environments, *Mater. Chem. and Phys.*, 104, pp. 125-132.

Eason, E. D.; Nelson, E. E. & Gilman, J. D. (1998), Modeling of Fatigue Crack Growth Rate for Ferritic Steels in Light Water Reactor Environments, *Nucl. Eng. and Des.*, 184, pp. 89-111.
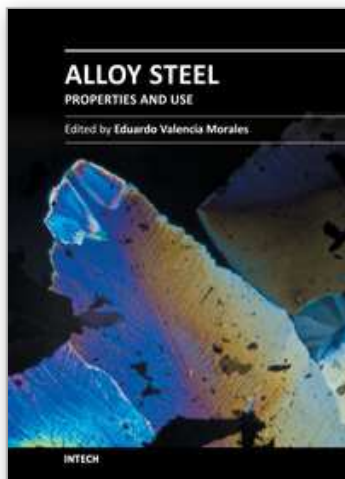
Alloy Steel - Properties and Use

Edited by Dr. Eduardo Valencia Morales

ISBN 978-953-307-484-9

Hard cover, 270 pages

Publisher InTech

Published online 22, December, 2011

Published in print edition December, 2011

The sections in this book are devoted to new approaches and usages of stainless steels, the influence of the environments on the behavior of certain classes of steels, new structural concepts to understand some fatigue processes, new insight on strengthening mechanisms, and toughness in microalloyed steels. The kinetics during tempering in low-alloy steels is also discussed through a new set-up that uses a modified Avrami formalism.

How to reference

In order to correctly reference this scholarly work, feel free to copy and paste the following:

J. Y. Huang, J. J. Yeh, J. S. Huang and R. C. Kuo (2011). Environmentally Assisted Cracking Behavior of Low Alloy Steels in Simulated BWR Coolant Conditions, Alloy Steel - Properties and Use, Dr. Eduardo Valencia Morales (Ed.), ISBN: 978-953-307-484-9, InTech, Available from: http://www.intechopen.com/books/alloy-steel-properties-and-use/environmentally-assisted-cracking-behavior-of-low-alloy-steels-in-simulated-bwr-coolant-conditions

INTECH
open science | open minds